Proc. Aachener Workshop 1996: Bildverarbeitung für die Medizin, Nov. 1996, T. Lehmann, I. Scholl, and K. Spitzer (Eds.), Verlag der Augustinus Buchhandlung 1996, pp. 41-46

Nonrigid Registration of Medical Images Based on Anatomical Point Landmarks and Approximating Thin-Plate Splines

K. Rohr[1], H.S. Stiehl[1], R. Sprengel[1], W. Beil[1], T.M. Buzug[2], J. Weese[2], and M.H. Kuhn[2]

[1] Universität Hamburg, Fachbereich Informatik, Arbeitsbereich Kognitive Systeme, Vogt-Kölln-Str. 30, D-22527 Hamburg, Germany
[2] Philips Research, Technical Systems Hamburg, Röntgenstr. 24-26, D-22335 Hamburg
rohr@informatik.uni-hamburg.de

Previous work on nonrigid registration of medical images based on thin-plate splines has concentrated on using interpolation schemes. Such schemes force the corresponding landmarks to exactly match each other and thus assume that the landmark positions are known exactly. However, in real applications the localization of landmarks is always prone to error. Therefore, to cope with these errors, we have investigated the application of an approximation scheme which is based on regularization theory. In addition to this study, we report on investigations into semi-automatic extraction of anatomical point landmarks of the human brain.

Keywords: Image Registration, Thin-Plate Splines, Anatomical Landmarks

1 Introduction

Registration (or matching) denotes the process in which two existing representations are put into correspondence. The aim is to find a transformation that describes the mapping between these two representations. Particularly, in neurosurgery and radiotherapy planning it is important to either register images from different modalities, e.g. CT (X-ray Computed Tomography) and MR (Magnetic Resonance) images, or to match images to atlas representations. If only *rigid* transformations were applied, then the accuracy of the resulting match often is not satisfactory w.r.t. clinical requirements. In general, *nonrigid* transformations are required to cope with the variations between the data sets.

This contribution is concerned with nonrigid registration of medical image data based on a set of corresponding anatomical point landmarks. Previous work on this topic has concentrated on i) selecting the corresponding landmarks manually and on ii) using an interpolating transformation model (Bookstein [1], Evans et al. [3], and Mardia and Little [6]). The basic approach draws upon thin-plate splines and is computationally efficient, robust, and general w.r.t. different types of images and atlases. Also, the approach is well-suited for user-interaction which is important in clinical scenaria. However, an interpolation scheme forces the corresponding landmarks to exactly match each other. The underlying assumption is that the landmark positions are known exactly. In real applications, however, the localization of landmarks is always prone to error. This is true for

interactive as well as for automatic landmark localization.

Therefore, to take into account these localization errors, we have investigated the application of an approximation scheme where the corresponding thin-plate splines result from regularization theory. Generally, such an approach yields a more accurate and robust registration result. In particular, outliers do not disturb the registration result as much as is the case with an interpolation scheme. Also, it is possible to individually weight the landmarks according to their localization uncertainty. We have applied this approach to nonrigid registration of tomographic images of the human brain.

Additionally, we report on first investigations toward the semi-automatic extraction of anatomical point landmarks using differential operators. Algorithms for this task are important since manual selection of landmarks is time-consuming and often lacks accuracy.

2 Clinical Applications for Nonrigid Registration

One possible application for nonrigid registration is trajectory planning for neurosurgical intervention. Pain treatment as well as epilepsy treatment sometimes require to localize a functionally important region not visible in the available image data. There are instructions available in the literature how to construct the position of such a region given landmarks which can be identified in CT or MR images. Hence, it is useful to superimpose an atlas with a medical image as already proposed by Talairach. Due to the individual variability of anatomical structures, rigid registration is generally not sufficient and nonrigid matching should be applied.

Another application is the registration of CT and MR images for the purpose of radiotherapy planning. Additionally, a template atlas can be superimposed on the MR image to indicate, for example, organs at risk. This superposition result is then overlayed on the CT image prior to dose calculation and isodose visualization on the MR image. It is questionable whether rigid registration is suitable for this purpose since MR images are geometrically distorted. On the one hand, scanner-induced distortions have to be coped with which are caused by, e.g., inhomogeneities of the main magnetic field, imperfect slice or volume selection pulses, nonlinearities of the magnetic field gradients, and eddy currents. These distortions can be reduced by suitable calibration steps: The inhomogeneities of the main magnetic field are minimized by passive and active shimming whereas, e.g., the gradient nonlinearities cannot be completely shimmed. Thus, depending on the scanner protocol, the sum of all remaining distortions leads to a residual error of a few millimeters (for a spherical field of view of 25 cm). On the other hand, there are geometrical distortions in MR images that are induced by the patient and cannot be removed by calibration. Parameters such as susceptibility variations, chemical shift of non-water protons and flow-induced distortions for vessels are very important. While the susceptibility difference of tissue and bone is negligible, the susceptibility difference between tissue and air is approximately 10^{-5}. This can result in a field variation of up to 10 ppm and geometrical distortions of more than 5 mm which is most important for the nasal and aural regions. Consequently, due to the scanner- as well as the patient-induced distortions of the MR image, CT and MR images in general cannot be satisfactorily registered using rigid transformations.

3 Thin-Plate Spline Approximation

The use of thin-plate spline interpolation for point-based registration of medical images was first proposed by Bookstein [1]. In this section, we extend this approach in such a way that we can take into account landmark localization errors. We achieve this by combining a quadratic approximation criterion with the original smoothness functional:

$$J_\lambda(\mathbf{u}) = \frac{1}{n}\sum_{i=1}^{n} |\mathbf{q}_i - \mathbf{u}(\mathbf{p}_i)|^2 + \lambda J_m^d(\mathbf{u}), \tag{1}$$

where n is the number of landmarks, d the dimension of the image, and m the order of derivatives in the smoothness functional (see Wahba [11] for a theoretical study of such functionals). The first term (data term) measures the distances between the transformed source landmarks $\mathbf{p}_i$ and the target landmarks $\mathbf{q}_i$. The second term measures the smoothness of the resulting transformation. Hence, the minimization of (1) yields a transformation $\mathbf{u}$, which i) approximates the distance of the source landmarks to the target landmarks and ii) is sufficiently smooth. The relative weight between the approximation behavior and the smoothness of the transformation is determined by the regularization parameter $\lambda > 0$. In the limit of $\lambda \to 0$ we obtain an interpolating transformation, whereas in the limit of $\lambda \to \infty$ we get a global polynomial of order up to $m-1$.

The solution to (1) can be stated analytically as the weighted sum of polynomials ϕ_j and certain radial basis functions U_i using the coefficient vectors $\mathbf{a}$ and $\mathbf{w}$. The computational scheme to compute $\mathbf{a}$ and $\mathbf{w}$ then reads as

$$\begin{aligned} (\mathbf{K} + n\lambda\mathbf{I})\mathbf{w} + \mathbf{P}\mathbf{a} &= \mathbf{v} \\ \mathbf{P}^T\mathbf{w} &= 0, \end{aligned} \tag{2}$$

where $K_{ij} = U_i(\mathbf{p}_j)$, $P_{ij} = \phi_j(\mathbf{p}_i)$, and $\mathbf{v}$ represents one component of the coordinates of the $\mathbf{q}_i$. The interesting fact is that this scheme is nearly the same as in the case of interpolation. We only have to add $n\lambda$ in the diagonal of the matrix $\mathbf{K}$.

A generalization of the approximation scheme can be attained, if information about the accuracy of the landmarks is available. Then, we can weight each single data term in (1) by the variance σ_i^2 (see [8], [9] for details). Note, that this approach can be applied to images of arbitrary dimension, i.e. in particular to 2D as well as 3D images.

4 Experimental Results

Within the scenario of CT-MR registration as discussed above we here consider the application of correcting patient-induced susceptibility distortions of MR images. To this end we have acquired two sagittal MR images of a healthy human volunteer brain with typical susceptibility distortions. In our experiment we used a high-gradient MR image as "ground truth" (instead of clinically common CT images) to avoid exposure of the volunteer to radiation. Both turbo-spin echo images have consecutively been acquired on a modified Philips $1.5T$ MR scanner with a slice thickness of $4mm$ without repositioning. Therefore, we are sure that we actually have identical slicing in space. Using a gradient of

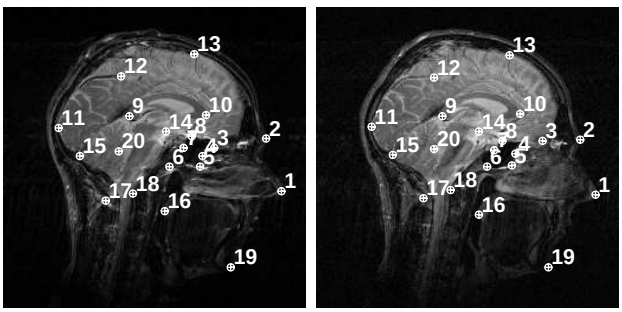

Figure 1: Original MR images with landmarks: First (left) and second (right) image.

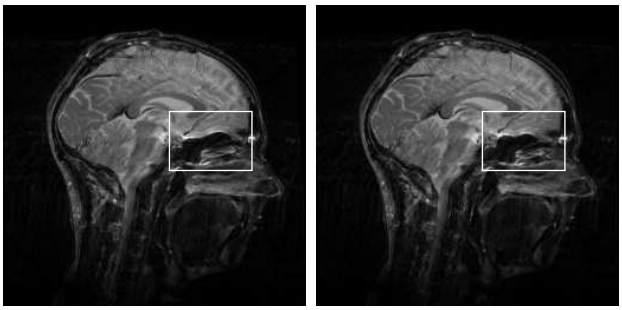

Figure 2: Registration results: Interpolation (left) and approximation (right).

$1mT/m$ and $6mT/m$ for the first and second image then leads to a shift of ca. 7.5...10mm and ca. 1.3...1.7mm, respectively.

Within each of the two images we have manually selected 20 point landmarks. To simulate outliers, one of the landmarks in the first image (No. 3) has been shifted about 15 pixels away from its true position for demonstration purposes (see Fig. 1). Note, however, that manual localization of landmarks actually can be prone to relatively large errors. Fig. 2 shows the results of the interpolating vs. the approximating thin-plate spline approach. Each result represents the transformed first image. It can be seen that the interpolation scheme yields a rather unrealistic deformation since it forces all landmark pairs, including the pair with the simulated outlier, to exactly match each other. Using our approximation scheme instead yields a more accurate registration result.

5 Semi-Automatic Landmark Localization

One main problem with point landmarks is their reliable and accurate extraction from 3D images. Therefore, 3D point landmarks have usually been selected manually (e.g., Evans et al. [3], Hill et al. [5]; but see also Thirion [10]). In this section, we briefly describe our first investigations into semi-automatic localization of 3D anatomical point landmarks. Semi-automatic means that either a region-of-interest (ROI) or an approximate position of a specific landmark (or both) is given by the user. Then, an algorithm has to provide a refined position of the landmark. Alternatively, landmark candidates for a large ROI or even for the whole data set may be provided automatically from which the final set of landmarks is selected manually. Such a semi-automatic approach has the advantage that

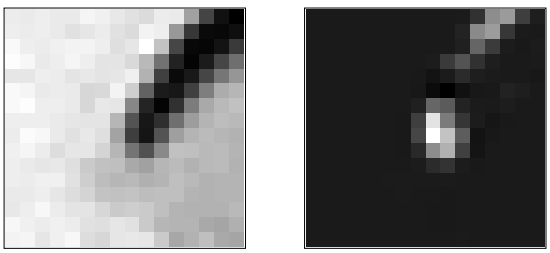

Figure 3: Right frontal horn in a 3D MR data set (left) and result of computing the 3D Gaussian curvature (right)

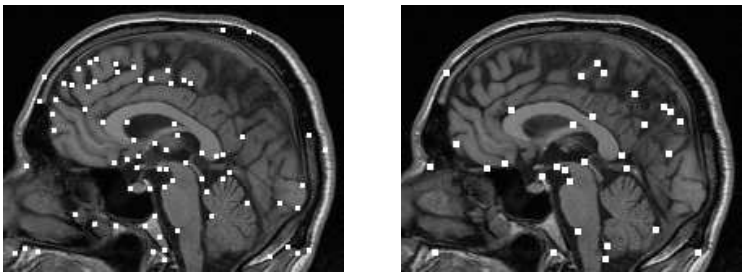

Figure 4: Landmark candidates: Application of a 2D 'corner' detector (left) vs. a 3D extension (right) on a 2D and 3D MR image, respectively.

a user has the possibility to control the results ("keep-the-user-in-the-loop").

Within a ROI we apply specific 3D differential operators such as to exploit the knowledge about a landmark as far as possible, in particular it's geometric structure. To localize curvature extrema we use an operator which estimates Gaussian curvature, i.e. the product of the two principal curvatures $K = \lambda_1\lambda_2$, multiplied with the fourth power of the gradient magnitude $|\nabla g|$. Fig. 3 shows a result of this operator for the right frontal horn in a 3D MR image. It can be seen that we obtain a strong operator response at the tip of the frontal horn.

We also investigate 3D differential operators which are extensions of existing 2D 'corner detectors'. For a recent analytic study of such 2D operators see Rohr [7]. These operators have the advantage that only low order partial derivatives of the image function are necessary (first or first and second order). Therefore, these operators are computationally efficient. As an example, in Fig. 4 we show the application of the 2D operator of Förstner [4] vs. a 3D extension of it: $det\underline{C}_g/trace\underline{C}_g \rightarrow max$, where $\underline{C}_g = \overline{\nabla g\,(\nabla g)^T}$ and ∇g denotes the image gradient in 2D and 3D, respectively. Note, that in the 2D case many well detected landmarks agree with the manually selected landmarks in Bookstein [2]. Note also, that the 3D operator actually takes into account the 3D structure of the landmarks and therefore in a single slice of a 3D image only a few of the 3D point landmarks are visible, i.e., other landmarks according to [2] have been detected in different slices.

Acknowledgement

Support of Philips Research Hamburg, project IMAGINE (IMage- and Atlas-Guided Interventions in NEurosurgery), is gratefully acknowledged.

References

[1] F. Bookstein. Principal warps: Thin-plate splines and the decomposition of deformations. *IEEE Trans. Pattern Anal. and Machine Intell.*, 11(6):567–585, 1989.

[2] F. Bookstein. Thin-plate splines and the atlas problem for biomedical images. In A. Colchester and D. Hawkes, editors, *12th Internat. Conf. Information Processing in Medical Imaging*, volume 511 of *Lecture Notes in Computer Science*, pages 326–342, Wye/UK, 1991. Springer Berlin Heidelberg.

[3] A. Evans, W. Dai, L. Collins, P. Neelin, and S. Marrett. Warping of a computerized 3-d atlas to match brain image volumes for quantitative neuroanatomical and functional analysis. In M. Loew, editor, *Medical Imaging V: Image Processing*, volume 1445 of *Proc. SPIE*, pages 236–246, San Jose, CA, 1991.

[4] W. Förstner. A feature based correspondence algorithm for image matching. *Intern. Arch. of Photogrammetry and Remote Sensing*, 26-3/3:150–166, 1986.

[5] D. Hill, D. Hawkes, J. Crossman, M. Gleeson, T. Cox, E. Bracey, A. Strong, and P. Graves. Registration of MR and CT images for skull base surgery using point-like anatomical features. *The British J. of Radiology*, 64(767):1030–1035, 1991.

[6] K. Mardia and J. Little. Image warping using derivative information. In F. Bookstein, J. Duncan, N. Lange, and D. Wilson, editors, *Mathematical Methods in Medical Imaging III*, volume 2299 of *Proc. SPIE*, pages 16–31, San Diego, CA, 25-26 July 1994.

[7] K. Rohr. Localization properties of direct corner detectors. *J. of Mathematical Imaging and Vision*, 4(2):139–150, 1994.

[8] K. Rohr, H. S. Stiehl, R. Sprengel, W. Beil, T. M. Buzug, J. Weese, and M. H. Kuhn. Point-based elastic registration of medical image data using approximating thin-plate splines. In K.-H. Höhne and R. Kikinis, editors, *4th Internat. Conf. Visualization in Biomedical Computing (VBC'96)*, volume 1131 of *Lecture Notes in Computer Science*, pages 297–306. Springer Berlin Heidelberg, 1996.

[9] R. Sprengel, K. Rohr, and H. S. Stiehl. Thin-plate spline approximation for image registration. In *18th Internat. Conf. of the IEEE Engineering in Medicine and Biology Society*, 1996. to appear.

[10] J.-P. Thirion. Extremal points: definition and application to 3d image registration. In *Proc. IEEE Conf. on Computer Vision and Pattern Recognition*, pages 587–592, Seattle/Washington, USA, 1994.

[11] G. Wahba. *Spline Models for Observational Data*. Society for Industrial and Applied Mathematics, Philadelphia, Pennsylvania, 1990.